

Published in final edited form as:

Arterioscler Thromb Vasc Biol. 2012 May ; 32(5): 1271–1279. doi:10.1161/ATVBAHA.112.246371.

A novel mRNA binding protein complex promotes localized plasminogen activator inhibitor-1 accumulation at the myoendothelial junction

Katherine R. Heberlein^{1,2}, Jenny Han³, Adam C. Straub¹, Angela K. Best¹, Christoph Kaun⁴, Johann Wojta⁴, and Brant E. Isakson^{1,2,*}

¹Robert M. Berne Cardiovascular Research Center, University of Virginia School of Medicine, P.O. Box 801394, Charlottesville, VA 22908 USA

²Department of Molecular Physiology and Biological Physics, University of Virginia School of Medicine, P.O. Box 801394, Charlottesville, VA 22908 USA

³Department of Pharmacology, University of Virginia School of Medicine, Vienna Austria

⁴Medical University of Vienna, Vienna Austria

Abstract

Objective—Plasminogen activator inhibitor-1 (PAI-1) has previously been shown to be key to the formation of myoendothelial junctions (MEJs) in normal and pathological states (e.g., obesity). We there for sought to identify the mechanism whereby PAI-1 could be selectively accumulated at the MEJ.

Methods and Results—We identified PAI-1 protein enrichment at the MEJ in obese mice and in response to TNF- α with a vascular cell co-culture. However, PAI-1 mRNA was also found at the MEJ and transfection with a PAI-1-GFP with TNF- α did not demonstrate trafficking of the protein to the MEJ. We there for hypothesized the PAI-1 mRNA was being locally translated and identified serpine binding protein-1, which stabilizes PAI-1 mRNA, as being enriched in obese mice and after treatment with TNF- α , while staufen, which degrades PAI-1 mRNA, was absent in obese mice and after TNF- α application. We identified nicotinamide phosphoribosyl transferase as a serpine binding protein-1 binding partner with a functional tau-like microtubule binding domain. Application of peptides against the microtubule binding domain significantly decreased the number of MEJs and the amount of PAI-1 at the MEJ.

Conclusions—We conclude that PAI-1 can be locally translated at the MEJ due to a unique mRNA binding protein complex.

Keywords

plasminogen activator inhibitor-1; myoendothelial junction; serpine binding protein-1 (SERBP1); Staufen; mRNA binding protein; nicotinamide phosphoribosyl transferase (NAMPT)

Introduction

The myoendothelial junction (MEJ) is a heterocellular junction located predominantly within the resistance vasculature and is comprised of vascular smooth muscle cells

* to whom correspondence should be addressed: brant@virginia.edu, T: 434-924-2093, F: 434-924-2828.

Disclosures

None.

(VSMCs) and endothelial cell (EC) extensions that extend from each cell type into the internal elastic lamina (IEL) and form a close apposition with the opposing cell membrane¹⁻³. The MEJ is presumed to be a highly organized signaling microdomain, acting as a conduit for heterocellular signaling within the vasculature⁴⁻⁷. Indeed, deregulation of the MEJ is associated with several disease states, but the mechanism for how these changes are occurring has not been fully described⁷. Most recently, changes in the formation of MEJs were shown to be regulated by plasminogen activator inhibitor-1 (PAI-1) at the MEJ⁴. The expression of PAI-1 directly affected MEJ formation both in vitro and in vivo, with potential effects on signaling between the two cell types⁴. However, despite its importance in MEJ formation, the mechanism for PAI-1 localization to the MEJ remains undefined.

Although a common means of achieving subcellular organization is through protein trafficking, recent focus has highlighted a role for localization of messenger RNA (mRNA)⁸, which suggests that the ability to localize a single transcript that acts as a template for translating several copies of the same protein may be more energy efficient for the cell⁹. Additionally, localized protein translation can facilitate the rapid accumulation of a protein in response to various stimuli^{9, 10}. For mRNA localization to occur, the transcript of interest is typically bound by an mRNA-binding protein (RBP), forming an mRNA-RBP complex, which is trafficked to the targeted area of a cell¹¹. Importantly, the mRNA-RBP complex must be stabilized or anchored to the cytoskeleton within the targeted area of the cell, in order to achieve asymmetrical distribution of the protein¹¹.

To test the hypothesis that PAI-1 localization to the MEJ can be achieved through localization of PAI-1 mRNA, we looked at the expression of PAI-1, as well as two RBPs, the PAI-1 mRNA stabilizing RBP, serpine binding protein-1 (SERBP1)^{12, 13} and Staufen, an RBP associated with PAI-1 mRNA degradation^{14, 15}, in response to inflammatory stimulation. We also looked at a novel role for the protein nicotinamide phosphoribosyl transferase (NAMPT; or PBEF/Visfatin¹⁶) as an anchoring component for the PAI-1 mRNA-RBP complex at the MEJ. In response to disease conditions, we show the first evidence for a PAI-1 mRNA localization mechanism to the MEJ. The increases in PAI-1 correlate with simultaneous increases in SERBP1 and NAMPT, which we suggest act together as a novel PAI-1 mRNA-RBP complex at the MEJ. Disrupting the ability of the complex to anchor at the MEJ inhibits PAI-1 localization to the MEJ and ultimately prevents the effects of TNF- α on MEJ formation. As the MEJ is hypothesized to play an integral role in the regulation of normal vascular function, understanding how its formation is regulated, especially during vascular disease states such as those associated with the metabolic syndrome, may provide valuable therapeutic targets in the future.

Methods

Mice

Wildtype mice, strain C57Bl/6 were males 8–10 weeks of age and used according to the University of Virginia Animal Care and Use Committee guidelines. Mice used for high fat comparison were C57Bl/6 mice fed a caloric-rich diet (5.45 kcal/g, 0.2% cholesterol, 35.5% fat; Bio-Serv).

Ultrastructure Electron Microscopy

Coronary arteries were fixed in 4% paraformaldehyde and 2.5% glutaraldehyde and ultrastructural TEM images were obtained as described¹⁷. The total number of MEJs within a vessel using a minimum of 5 TEM images per coronary arteriole was quantified as previously described⁴. Briefly, the radial length of a vessel was measured using calibrated Metamorph software. Numbers represent the average number of MEJs per 10 μ m radial

length \pm SE. A minimum radial diameter of 150 μ m per mouse and 10 μ m between each TEM section were used.

Vascular cell-co-culture

Vascular cell co-cultures (VCCC) were assembled as described¹⁸. Cells were derived from human coronary artery (Lonza, Walkersville). Endothelial cells were grown in MCDB131 (Gibco), supplemented with EC Lonza bullet kits (Lonza), while VSMC were grown in DMEM F/12 (Gibco) supplemented with VSMC Lonza bullet kits (Lonza). Seeding densities of 7.5×10^4 VSMC and 3.6×10^5 EC were used. Recombinant human tumor necrosis factor- α (TNF- α ; 10ng/mL; R&D Systems) was added 18 hours before isolation. Peptides with a sequence directed against the microtubule binding domain of NAMPT (MKQKMWSIENIAFGSGGG) or a scrambled sequence (GSQSGNMEFGIMAKGWKIC) with a HIV-derived TAT sequence (each at 1 mg/mL; Anaspec) were added concurrently with TNF- α 18 hours before isolation.

Isolation of MEJ fractions

In vitro VCCC fractions were collected as previously described⁴. Briefly, VSMC and EC monolayers were scraped into lysis buffer. The MEJ fractions were collected by vortexing the denuded membrane in lysis buffer. Fractions for immunoblot analysis were sonicated and spun at $500 \times g$ for 5 minutes and the supernatant collected. Fractions for co-immunoprecipitations were disrupted using a douncer and spun at $500 \times g$ for 5 minutes and the supernatant collected. All steps were performed at 4°C. The RNA extraction and cDNA preparation from isolated VCCC fractions was performed according to the RNeasy® 96 protocol (Qiagen). The real-time PCR was performed as previously described¹⁹. Primer design was done using Roche Universal ProbeLibrary Assay Design Center, PAI-1 UPL probe #15; Amplicon Size (bp) 102–OSM [forward primer: 5'-tccagcagctgaattcctg-3', reverse primer: 5'-gctggagacatctgcatcct-3']. GAPDH UPL probe #60; Amplicon Size (bp) 66–OSM [forward primer: 5'agccacatcgctcagacac-3', reverse primer: 5'-gcccaatagaccaaatcc-3']. Data was analyzed using LightCycler Software Version 3.5 (Roche, Basel, Switzerland). PAI-1 antigen in each cell fraction was measured using ELISAS for total and active PAI-1, as previously described¹⁹ (Technoclone, Vienna, Austria). All measurements were performed in triplicate.

Antibodies and Protein

Secondary antibodies: phalloidin conjugated to Alexa 488 or Alexa 594, donkey anti-rabbit or donkey anti-mouse Alexa 488 or Alexa 594, all from Invitrogen. Goat anti-rabbit or anti-mouse IRDye 680 or 800CW was used for immunoblots (Li-cor Biosciences). Primary antibodies: PAI-1 polyclonal, SERBP1 monoclonal, Staufen monoclonal and PBEF monoclonal (all from Abcam), GAPDH (monoclonal, Zymed). Anti-rabbit and anti-mouse 10 nm gold beads and anti-mouse 15 nm gold beads were from Electron Microscopy Services.

Immunoblots

Protein fractions were run on 10% SDS-PAGE Gels, transferred to nitrocellulose and imaged on a Li-Cor Odyssey Imager¹⁷. In most cases, because GAPDH is highly ubiquitous in both the membrane and cytosolic fraction of a cell²⁰, GAPDH was used to normalize to protein expression as it is consistent between each protein fraction, as we have previously demonstrated⁴ and loads identically to beta tubulin, a cytoskeletal loading protein (Supplemental Figure I).

Co-immunoprecipitation

Co-immunoprecipitations were performed as previously described²¹. Briefly, SERBP1 or NAMPT antibody was conjugated to Mouse IgG/IgM Dynabeads (Invitrogen) and incubated with equal amounts of EC, VSMC, or MEJ fractions isolated from the VCCC, as determined by a Bradford protein assay. The fractions were run on an SDS-PAGE gel, transferred to nitrocellulose and imaged on a Li-Cor Odyssey Imager.

Immunostaining

Immunohistochemistry on the VCCC was performed as described²². For all micrographs, VCCC are arranged with the EC monolayer above the VSMC monolayer.

Quantification of MEJs using the VCCC

Quantification of in vitro MEJs was performed as described⁴.

Immunolabeling on TEM Sections

Visualization and quantification of proteins by TEM immunolabeling was performed as described²⁵.

Generation of GFP-tagged PAI-1 construct

The full length PAI-1 sequence (Origene) was cloned into a pEGFP-C1 expression vector (kindly provided by Dr. Doug Bayliss, University of Virginia) and validated by sequencing.

Transfections

For transfections, ECs were transferred to a cuvette containing 100 μ l of Amaxa Nucleofector solution (Lonza) with 5 μ g of the GFP-tagged PAI-1 construct. The cuvette was placed in the Nucleofector cuvette holder and subjected to electroporation (EC transfection program, S-005). Following electroporation, the ECs were plated on VCCCs as per normal protocol (see above).

Microtubule binding assay

Microtubules were assembled per manufacturer specifications (Cytoskeleton, Inc.). The microtubules were incubated with purified recombinant visfatin (rNAMPT), BSA or a cocktail mix of microtubule associated proteins. The reactions were layered onto a cushion buffer and centrifuged at 100,000 \times g at room temperature for 40 minutes. The uppermost layer of supernatant and pellet were resuspended in 10 μ l of 5x or 50 μ l of 1x laemmli buffer, respectively. The samples were run on 10% SDS-PAGE gels and proteins were detected by immunoblot analysis or coomassie stain⁴.

2D-DIGE Analysis

Analysis was performed as previously described⁴.

Mass Spectrometry

Protein identification was performed as previously described⁴.

Statistics

Significance for all experiments was at $P < 0.05$ and determined by one-way ANOVA (Bonferroni post hoc test), unless otherwise denoted; error bars are \pm SE using Origin Pro 6.0 software.

Results

Previous data has shown that in response to a high fat diet, there is a significant increase in MEJ formation, as well as systemic expression of PAI-1, *in vivo*.⁴ To verify that these increases in MEJ formation correlated with an increase in PAI-1 specifically at the MEJ, we performed transmission electron microscopy (TEM) analysis with immunogold labeling for PAI-1. Quantified immunolabeling for PAI-1 on isolated coronary arteries from C57Bl/6 mice on a normal or high fat diet shows that there is a significant increase in PAI-1 protein expression at the MEJ in response to high fat diet (Figure 1A, Supplemental Figure II). To further elucidate the mechanism for PAI-1 localization at the MEJ in response to a high fat diet, we used an *in vitro* model of the MEJ, the vascular cell co-culture (VCCC)^{4, 18, 22}, and treated the ECs with TNF- α to increase PAI-1^{23, 24} and mimic the low level chronic inflammatory conditions of a high fat diet and metabolic syndrome^{25, 26}. High glucose, an inflammatory-independent stimuli to increase PAI-1²⁷ did not show increases in PAI-1 confined to MEJs (Supplemental Figure III). We confirmed the ability of TNF- α to mimic a high fat diet, showing there was a significant increase in MEJ formation *in vitro* (Figure 1B), and used PAI-1 specific ELISAs for both total and active PAI-1 to show an increase in PAI-1 protein especially at the MEJ, as compared to EC or VSMC fractions (Figure 1C). To determine if the increase in PAI-1 at the MEJ was the result of protein trafficking, we transfected ECs with a GFP-tagged PAI-1 construct prior to culturing the cells on the VCCC. Movement of the GFP-tagged PAI-1 in response to TNF- α was monitored using quantitative immunoblot analysis, comparing endogenous and GFP-tagged PAI-1 expression at the MEJ (Figure 1D). Because we detected no increase in GFP-tagged PAI-1 at the MEJ following treatment with TNF- α , this suggested that the enrichment of PAI-1 at the MEJ in response to inflammatory conditions was not due to a protein trafficking mechanism. For this reason, we used quantitative rt-PCR on isolated EC, VSMC and MEJ fractions and showed there was a global and significant increase in PAI-1 mRNA for all three cell fractions, in response to TNF- α (Figure 1E). In conjunction with this data, as well as previous work demonstrating rough endoplasmic reticulum at the MEJ (e.g.,^{6, 22} and Supplementary Figure IV), and the PAI-1 specific ELISAs, these data suggested there was a mechanism promoting the stabilization of PAI-1 mRNA at the MEJ in order to facilitate a local increase in PAI-1 protein in response to TNF- α .

In order to confirm a role for mRNA localization of PAI-1 at the MEJ, we verified the expression of the PAI-1 RBP, SERBP1, which has been demonstrated to stabilize PAI-1 mRNA^{12, 13}, using immunohistochemistry on transverse sections of the VCCC (Figure 2A) and quantitative immunoblots on isolated VCCC fractions (Figure 2B). In response to TNF- α there was a significant increase in SERBP1 expression at the MEJ *in vitro* (Figure 2A,B). Furthermore, using quantified immunolabeling for SERBP1 by TEM analysis, we verified the expression of SERBP1 at the MEJ *in vivo* and showed there was a significant increase in SERBP1 at the MEJ in response to a high fat diet (Figure 2C). Additionally, we looked at expression of the RBP, Staufen, which has been associated with the degradation of PAI-1 mRNA^{14, 15}. Using immunohistochemistry on transverse sections of the VCCC (Figure 2D) and quantified immunoblots from isolated VCCC fractions (Figure 2E), we show that in response to TNF- α , there was a significant decrease in Staufen expression at the MEJ *in vitro* (Figure 2F). These data suggested that in response to inflammatory conditions that mimic the metabolic syndrome, there is an organization of RBPs that associate with the stabilization of PAI-1 mRNA at the MEJ *in vitro* and *in vivo*.

Localization of mRNA requires that the mRNA-RBP complex be anchored to the targeted area within a cell, usually to the cytoskeleton. Although SERBP1 does not contain a cytoskeletal binding domain, proteomic analysis of the *in vitro* MEJs indicated that the protein nicotinamide phosphoribosyl transferase (NAMPT) which contains a conserved

microtubule binding domain (MBD) is highly enriched at the MEJ (Figure 3A). Using quantified immunoblots, there was a significant increase in NAMPT expression in response to inflammatory conditions at the MEJ, *in vitro* (Figure 3B) and *in vivo* using TEM immunolabeling for NAMPT on isolated coronaries (Figure 3C). Because NAMPT and SERBP1 expressions are similar in response to inflammatory conditions, we hypothesized that NAMPT may play a role as an anchoring component for a PAI-1 RBP complex with SERBP1, via its MBD. Using a microtubule binding assay to determine the ability of NAMPT to bind microtubules, we showed that purified recombinant NAMPT (rNAMPT) precipitated with microtubules when centrifuged together, indicating there was a strong interaction between NAMPT and microtubules (Figure 3D). Control experiments done in parallel support the interaction, showing that on its own, rNAMPT does not precipitate (Supplemental Figure V). To further confirm a role for NAMPT as an anchoring component of a PAI-1 RBP complex, we used immunohistochemistry on transverse sections of the VCCC co-labeled for SERBP1 and NAMPT. In response to TNF- α , SERBP1 and NAMPT colocalized together at the MEJ (Figure 4A). We next used isolated VCCC fractions and show both SERBP1 and NAMPT co-immunoprecipitated together in the MEJ fractions, and this interaction was enhanced in response to TNF- α (Figure 4B). Dual immunostaining for SERBP1 and NAMPT on TEM sections from isolated mouse coronary arteries further supported a role for NAMPT as part of the PAI-1 RBP complex, again showing a colocalization of the two proteins at the MEJ in response to a high fat diet (Figure 4C). Lastly, quantification of the distance between NAMPT and SERBP1 at the MEJs of coronary arteries showed a significant decrease in distance under high fat conditions (Figure 4D).

To confirm the importance of mRNA localization of PAI-1 at the MEJ, we designed a TAT-tagged peptide designed against the MBD of NAMPT and treated ECs of the VCCC to inhibit the ability of NAMPT to anchor the PAI-1 mRNA-RBP complex to microtubules at the MEJ. Quantified immunoblots for PAI-1 on isolated MEJ fractions show that in response to TNF- α or TNF- α plus a scrambled peptide, there is a significant increase in PAI-1 expression at the MEJ (Figure 5A). However, in the presence of the MBD peptide and TNF- α , there was no change in PAI-1 expression as compared to non-treated samples (Figure 5A), confirming the importance of PAI-1 mRNA trafficking in the accumulation of PAI-1 protein at the MEJ. It has previously been shown that PAI-1 expression regulates MEJ formation⁴. Therefore, using the same experimental conditions, we also show that by disrupting the microtubule binding capacity of NAMPT, we also inhibit the affects of TNF- α on MEJ formation as well (Figure 5B).

Discussion

In the present study, we provide evidence for a novel PAI-1 mRNA localization mechanism and highlight its importance in the regulation of MEJ formation in response to inflammatory conditions that are typical of the metabolic syndrome. The MEJ is reported to be a key component for the maintenance of normal vascular function and it has been suggested that changes in the regulation of the MEJ may play an important role in the progression of vascular disease (for review, see⁷). Indeed, recent evidence now shows there is a significant increase in MEJ formation in mice fed a high fat diet⁴ and that the changes in MEJ formation directly correlated with changes in PAI-expression *in vivo* and *in vitro*⁴. Importantly, although the previous work from our lab showed a novel role for PAI-1 I the regulation of MEJ formation, the mechanism by which PAI-1 accumulated at the MEJ in response to a high fat diet remained undefined. We now show that the significant increases in systemic PAI-1 seen in a high fat diet⁴ are also seen at the subcellular level, where there is a significant increase in PAI-1 protein at the MEJ *in vivo*, as compared to ECs or VSMCs

(Figure 1). These data suggested that in response to inflammatory conditions, there is a mechanism promoting a preferential increase in PAI-1 protein at the MEJ.

The accumulation of protein within a targeted area of a cell is likely accomplished by one of two mechanisms. Protein localization is either achieved by trafficking the protein of interest or trafficking of the mRNA for localized translation of the protein of interest, an important mechanism for subcellular organization of neurons²⁸. In order to identify the mechanism of PAI-1 localization to the MEJ, we chose to recapitulate the inflammatory state as seen in a high fat diet in vitro using the VCCC. Treating the endothelial cells with a low dose of TNF- α to mimic the inflammatory conditions in vivo²⁹ resulted in a significant increase in MEJ formation (Figure 1). When assessing the effects of TNF- α on PAI-1 expression in vitro, there was a global increase in PAI-1 protein and mRNA for all three VCCC fractions. However, despite TNF- α inducing a significant increase in PAI-1 mRNA in all three cell fractions, the fold increase in PAI-1 protein was greatest in the MEJ fractions (Figure 1). As such, there appeared to be a mechanism promoting the asymmetric accumulation of PAI-1 protein at the MEJ. Interestingly, although there are several mechanisms that can promote a global increase in PAI-1 protein³⁰, the mechanism of PAI-1 localization to the MEJ appears to be a specialized response to inflammatory stimulation, as increases in glucose do not result in increased PAI-1 at the MEJ (Supplemental Figure III).

To further elucidate the mechanism for increased PAI-1 expression at the MEJ, we designed a GFP-tagged PAI-1 construct in order to track the movement of PAI-1 in response to TNF- α . If PAI-1 localization was the result of protein trafficking, there would be a significant increase in GFP-tagged PAI-1 protein at the MEJ, in vitro. It is important to note that the GFP-tagged construct does not contain an NF- κ B promoter, which is the general mediator for TNF- α induced increases in PAI-1²⁴. Therefore, any increases in GFP at the MEJ would be the result of protein trafficking and not increased GFP-tagged protein production. Interestingly, despite a significant increase in endogenous PAI-1 protein, there was no increase in GFP-tagged PAI-1 at the MEJ, following exposure to TNF- α (Figure 1D). These data suggested that protein trafficking was not playing an important role in mediating PAI-1 localization to the MEJ, but rather the increases in PAI-1 protein at the MEJ were the result of a novel mRNA localization mechanism, promoting the stabilization of PAI-1 mRNA at the MEJ. Although these results do not negate additional mechanisms for PAI-1 localization to the MEJ, our results seem to suggest that in response to TNF- α , there is no movement of intracellular PAI-1 protein to the MEJ. Subcellular organization of signaling microdomains is an important facet of the mRNA localization mechanism, that translational machinery is also present within the targeted area of a cell. Recent data showed the classical TEM evidence for the presence of ribosomes and endoplasmic reticulum in the MEJ⁶, thereby supporting the ability for localized protein production at the MEJ. From this, we hypothesized that in response to disease conditions; the cell establishes an environment that promotes the stabilization of PAI-1 mRNA within the MEJ, resulting in increased PAI-1 protein at the MEJ.

The stabilization of a transcript is achieved through binding of the mRNA by an RBP and this mRNA-RBP complex anchors to the cytoskeleton within the targeted area of the cell, facilitating protein expression¹¹. Equally as important in targeted protein accumulation is mRNA degradation. Of interest, the PAI-1 transcript can be regulated by two separate RBPs, and occurs when the transcript is bound by the PAI-1 RBP, SERBP1^{12, 13}, while conversely, a separate RBP Staufen, has been shown to promote the degradation of PAI-1 mRNA when its expression is increased^{14, 15}. Given the role for each of these proteins in the regulation of PAI-1 mRNA, we hypothesized that in response to TNF- α or a high fat diet, there would be an increase in SERBP1 at the MEJ, in concurrence with a decrease in Staufen. This organization of proteins would create a subcellular microdomain that supports an increase in

PAI-1 mRNA and protein at the MEJ. Indeed, both in vitro and in vivo, there appears to be a distinct distribution of the two RBPs in response to inflammatory stimulation, where SERBP1 is increased at the MEJ and Staufen is decreased (Figure 2). However, it is important to note that although SERBP1 appears to play an important role in the stabilization of PAI-1 mRNA at the MEJ, it does not have the ability to anchor the mRNA-RBP complex to the cytoskeleton at the MEJ. Therefore, in order for the localization to be maintained, the PAI-1 mRNA-RBP complex requires an additional constituent to act as an anchoring protein.

Recent proteomic analysis of in vitro MEJs revealed a number of proteins whose expression levels were enriched at the MEJ under normal conditions⁴. Interestingly, the protein NAMPT was not only identified as having increased expression at the MEJ, but also contains a conserved microtubule binding domain, similar to the microtubule associated protein, tau³¹. Importantly, this provides NAMPT with the ability to anchor to microtubules, especially within the MEJ. In addition to being enriched at the MEJ, NAMPT expression is increased in several inflammatory disease states in which both PAI-1 and MEJ formation are also increased, such as obesity and diabetes^{4, 7, 32-36}. More specifically, it was recently shown that the protein levels of NAMPT and PAI-1 are positively correlated³². Together with the identification of the conserved MBD, these data suggested there may be a potential role for NAMPT as a crucial anchoring component of the PAI-1 RBP complex in response to inflammatory conditions. Furthermore, the ability of NAMPT to act as an anchoring component for the PAI-1 RBP complex is dependent on its capacity to interact with microtubules and we used a microtubule binding assay³⁷ to demonstrate a strong and novel interaction between NAMPT and microtubules, that is independent of microtubule length (Figure 3). It is interesting then, to speculate that by being independent of microtubule length, the interaction between NAMPT and microtubules may occur at the ends of microtubules, which would allow for stabilization of the complex well within the MEJ, close to the leading edge of the cellular extensions. As PAI-1 is a protein that is readily secreted³⁰, this may facilitate the rate of PAI-1 production and secretion at the MEJ, to promote timely increases in MEJ formation in response to inflammatory stimulation.

As an anchoring component for a PAI-1 RBP complex, NAMPT is not only required to interact with the cytoskeleton, but with the additional components of the RBP complex as well. Based on its ability interact with microtubules, we therefore sought to confirm an interaction between NAMPT and SERBP1. Immunolabeling for SERBP1 and NAMPT in vitro and in vivo, coupled with co-immunoprecipitation of the two proteins at the MEJ, strongly supported an interaction was occurring between the PAI-1 RBP SERBP and the protein NAMPT. Taken together with the microtubule binding assay, it is likely that NAMPT is acting as an anchoring component for the PAI-1 RBP complex at the MEJ.

Importantly, as NAMPT appears to be pleiotropic in function^{16, 36, 38}, it is unlikely that all NAMPT found at the MEJ is acting as an anchoring component for the PAI-1 RBP complex. Therefore, it becomes necessary to distinguish how NAMPT is regulated, especially in response to inflammatory conditions. Recent evidence now suggests that protein organization and function within the MEJ is facilitated by post-translational modifications on the protein of interest⁶. It is therefore possible that the regulation of NAMPT activity may also be achieved in part by post-translational modifications, specifically within the MBD. Indeed, the protein tau contains three MBDs (that are conserved with NAMPT) and binding of tau to microtubules is regulated by phosphorylation of these domains^{39, 40}. Specifically, the hyperphosphorylation of critical serine/threonines in the MBDs, decreases the affinity of tau for microtubule binding³⁹⁻⁴¹. Future investigation may show that the same is true for NAMPT and that differential phosphorylation of the NAMPT MBD might also

play a role in determining the intracellular function of NAMPT, in response to different stimuli.

Previous work from our lab has shown that PAI-1 expression and activity is crucial for the regulation of MEJ formation⁴. Therefore, if localization of PAI-1 mRNA is required for creating an asymmetric distribution of PAI-1 at the MEJ, disrupting the PAI-1 mRNA localization mechanism should inhibit the effects of inflammation on MEJ formation. When the microtubule binding capacity of NAMPT was blocked, TNF- α appeared to have no effect on PAI-1 expression at the MEJ (Figure 5). In sum, these data indicate there is an important role for the localization of PAI-1 mRNA in the mediation of MEJ formation during a pathological response (Figure 6). By disrupting the ability of the complex to anchor within the MEJ, the effects of inflammation on PAI-1 expression and MEJ formation can be reduced and thereby presents a future therapeutic target for vascular diseases that are also part of a larger metabolic syndrome.

Supplementary Material

Refer to Web version on PubMed Central for supplementary material.

Acknowledgments

We thank the University of Virginia Histology Core for sectioning and Jan Redick and Stacey Guillot at the University of Virginia Advanced Microscopy Core.

Source of Funding

This work was supported by National Institutes of Health grant HL088554 (B.E.I.), American Heart Association Scientist Development Grant (B.E.I.), an American Heart Association predoctoral fellowship (K.R.H.), and a National Research Science Award postdoctoral fellowship from the National Institutes of Health (A.C.S.)

References Cited

1. Rhodin JA. The ultrastructure of mammalian arterioles and precapillary sphincters. *J Ultrastruct Res.* 1967; 18:181–223. [PubMed: 5337871]
2. Sandow SL, Hill CE. Incidence of myoendothelial gap junctions in the proximal and distal mesenteric arteries of the rat is suggestive of a role in endothelium-derived hyperpolarizing factor-mediated responses. *Circ Res.* 2000; 86:341–346. [PubMed: 10679487]
3. Taugner R, Kirchheim H, Forssmann WG. Myoendothelial contacts in glomerular arterioles and in renal interlobular arteries of rat, mouse and tupaia belangeri. *Cell Tissue Res.* 1984; 235:319–325. [PubMed: 6705035]
4. Heberlein KR, Straub AC, Best AK, Greyson MA, Looft-Wilson RC, Sharma PR, Meher A, Leitinger N, Isakson BE. Plasminogen activator inhibitor-1 regulates myoendothelial junction formation. *Circulation Research.* 2010; 106:1092–1102. [PubMed: 20133900]
5. Straub AC, Johnstone SR, Heberlein KR, Rizzo MJ, Best AK, Boitano S, Isakson BE. Site-specific connexin phosphorylation is associated with reduced heterocellular communication between smooth muscle and endothelium. *J Vasc Res.* 2009; 47:277–286. [PubMed: 20016202]
6. Straub AC, Billaud M, Johnstone SR, Best AK, Yemen S, Dwyer ST, Looft-Wilson R, Lysiak JJ, Gaston B, Palmer L, Isakson BE. Compartmentalized connexin 43 s-nitrosylation/denitrosylation regulates heterocellular communication in the vessel wall. *Arteriosclerosis, Thrombosis, and Vascular Biology.* 2011; 31:399–407.
7. Heberlein KR, Straub AC, Isakson BE. The myoendothelial junction: Breaking through the matrix? *Microcirculation.* 2009:1–16.
8. Lecuyer E, Yoshida H, Parthasarathy N, Alm C, Babak T, Cerovina T, Hughes TR, Tomancak P, Krause HM. Global analysis of mRNA localization reveals a prominent role in organizing cellular architecture and function. *Cell.* 2007; 131:174–187. [PubMed: 17923096]

9. Du TG, Schmid M, Jansen RP. Why cells move messages: The biological functions of mRNA localization. *Semin Cell Dev Biol.* 2007; 18:171–177. [PubMed: 17398125]
10. Lawrence JB, Singer RH. Intracellular localization of messenger RNAs for cytoskeletal proteins. *Cell.* 1986; 45:407–415. [PubMed: 3698103]
11. Jansen RP. mRNA localization: Message on the move. *Nat Rev Mol Cell Biol.* 2001; 2:247–256. [PubMed: 11283722]
12. Heaton JH, Dlakic WM, Dlakic M, Gelehrter TD. Identification and cDNA cloning of a novel RNA-binding protein that interacts with the cyclic nucleotide-responsive sequence in the type-1 plasminogen activator inhibitor mRNA. *J Biol Chem.* 2001; 276:3341–3347. [PubMed: 11001948]
13. Tillmann-Bogush M, Heaton JH, Gelehrter TD. Cyclic nucleotide regulation of pai-1 mRNA stability. Identification of cytosolic proteins that interact with an A-rich sequence. *J Biol Chem.* 1999; 274:1172–1179. [PubMed: 9873066]
14. Gong C, Maquat LE. lncRNAs transactivate STAU1-mediated mRNA decay by duplexing with 3' UTRs via Alu elements. *Nature.* 2011; 470:284–288. [PubMed: 21307942]
15. Kim YK, Furic L, Parisien M, Major F, DesGroseillers L, Maquat LE. Staufen1 regulates diverse classes of mammalian transcripts. *EMBO J.* 2007; 26:2670–2681. [PubMed: 17510634]
16. Sommer G, Garten A, Petzold S, Beck-Sickingler AG, Bluher M, Stumvoll M, Fasshauer M. Visfatin/pbef/nampt: Structure, regulation and potential function of a novel adipokine. *Clin Sci (Lond).* 2008; 115:13–23. [PubMed: 19016657]
17. Johnstone SR, Ross J, Rizzo MJ, Straub AC, Lampe PD, Leitinger N, Isakson BE. Oxidized phospholipid species promote in vivo differential cx43 phosphorylation and vascular smooth muscle cell proliferation. *Am J Pathol.* 2009; 175:916–924. [PubMed: 19608875]
18. Isakson BE, Duling BR. Heterocellular contact at the myoendothelial junction influences gap junction organization. *Circ Res.* 2005; 97:44–51. [PubMed: 15961721]
19. Demyanets S, Kaun C, Rychli K, Rega G, Pfaffenberger S, Afonyushkin T, Bochkov VN, Maurer G, Huber K, Wojta J. The inflammatory cytokine oncostatin M induces pai-1 in human vascular smooth muscle cells in vitro via pi 3-kinase and erk1/2-dependent pathways. *Am J Physiol Heart Circ Physiol.* 2007; 293:H1962–1968. [PubMed: 17604327]
20. Rockstroh M, Muller SA, Jende C, Kerzhner A, von Bergen M, Tomm JM. Cell fractionation - an important tool for compartment proteomics. *Journal of Integrated Omics.* 2011; 1:135–143.
21. Billaud M, Lohman AW, Straub AC, Looft-Wilson R, Johnstone SR, Araj CA, Best AK, Chekeni FB, Ravichandran KS, Penuela S, Laird DW, Isakson BE. Pannexin1 regulates alpha1-adrenergic receptor-mediated vasoconstriction. *Circulation Research.* 2011; 109:80–85. [PubMed: 21546608]
22. Isakson BE, Ramos SI, Duling BR. Ca²⁺ and inositol 1,4,5-trisphosphate-mediated signaling across the myoendothelial junction. *Circ Res.* 2007; 100:246–254. [PubMed: 17218602]
23. Macfelda K, Weiss TW, Kaun C, Breuss JM, Zorn G, Oberndorfer U, Voegele-Kadletz M, Huber-Beckmann R, Ullrich R, Binder BR, Losert UM, Maurer G, Pacher R, Huber K, Wojta J. Plasminogen activator inhibitor 1 expression is regulated by the inflammatory mediators interleukin-1alpha, tumor necrosis factor-alpha, transforming growth factor-beta and oncostatin M in human cardiac myocytes. *J Mol Cell Cardiol.* 2002; 34:1681–1691. [PubMed: 12505065]
24. Hou B, Eren M, Painter CA, Covington JW, Dixon JD, Schoenhard JA, Vaughan DE. Tumor necrosis factor alpha activates the human plasminogen activator inhibitor-1 gene through a distal nuclear factor kappaB site. *J Biol Chem.* 2004; 279:18127–18136. [PubMed: 14963043]
25. Catalan V, Gomez-Ambrosi J, Ramirez B, Rotellar F, Pastor C, Silva C, Rodriguez A, Gil MJ, Cienfuegos JA, Fruhbeck G. Proinflammatory cytokines in obesity: Impact of type 2 diabetes mellitus and gastric bypass. *Obes Surg.* 2007; 17:1464–1474. [PubMed: 18219773]
26. Vykoukal D, Davies MG. Vascular biology of metabolic syndrome. *J Vasc Surg.* 2011; 54:819–31. [PubMed: 21439758]
27. Maiello M, Boeri D, Podesta F, Cagliero E, Vichi M, Odetti P, Adezati L, Lorenzi M. Increased expression of tissue plasminogen activator and its inhibitor and reduced fibrinolytic potential of human endothelial cells cultured in elevated glucose. *Diabetes.* 1992; 41:1009–1015. [PubMed: 1628760]
28. Donnelly CJ, Fainzilber M, Twiss JL. Subcellular communication through RNA transport and localized protein synthesis. *Traffic.* 2010; 11:1498–1505. [PubMed: 21040295]

29. Picchi A, Gao X, Belmadani S, Potter BJ, Focardi M, Chilian WM, Zhang C. Tumor necrosis factor-alpha induces endothelial dysfunction in the prediabetic metabolic syndrome. *Circ Res*. 2006; 99:69–77. [PubMed: 16741160]
30. Lijnen HR. Pleiotropic functions of plasminogen activator inhibitor-1. *J Thromb Haemost*. 2005; 3:35–45. [PubMed: 15634264]
31. Lee G, Neve RL, Kosik KS. The microtubule binding domain of tau protein. *Neuron*. 1989; 2:1615–1624. [PubMed: 2516729]
32. Malavazos AE, Ermetici F, Cereda E, Coman C, Locati M, Morricone L, Corsi MM, Ambrosi B. Epicardial fat thickness: Relationship with plasma visfatin and plasminogen activator inhibitor-1 levels in visceral obesity. *Nutr Metab Cardiovasc Dis*. 2008; 18:523–530. [PubMed: 18083357]
33. Retnakaran R, Youn BS, Liu Y, Hanley AJ, Lee NS, Park JW, Song ES, Vu V, Kim W, Tungtrongchitr R, Havel PJ, Swarbrick MM, Shaw C, Sweeney G. Correlation of circulating full-length visfatin (pbeif/nampt) with metabolic parameters in subjects with and without diabetes: A cross-sectional study. *Clin Endocrinol (Oxf)*. 2008; 69:885–893. [PubMed: 18410550]
34. Fain JN, Tagele BM, Cheema P, Madan AK, Tichansky DS. Release of 12 adipokines by adipose tissue, nonfat cells, and fat cells from obese women. *Obesity (Silver Spring)*. 2010; 18:890–896. [PubMed: 19834460]
35. Wang BW, Lin CM, Wu GJ, Shyu KG. Tumor necrosis factor-alpha enhances hyperbaric oxygen-induced visfatin expression via jnk pathway in human coronary arterial endothelial cells. *J Biomed Sci*. 2011; 18:27. [PubMed: 21542902]
36. Wang P, Vanhoutte PM, Miao CY. Visfatin and cardio-cerebro-vascular disease. *J Cardiovasc Pharmacol*. 2012; 59:1–9. [PubMed: 21266913]
37. Sontag E, Nunbhakdi-Craig V, Lee G, Brandt R, Kamibayashi C, Kuret J, White CL 3rd, Mumby MC, Bloom GS. Molecular interactions among protein phosphatase 2a, tau, and microtubules. Implications for the regulation of tau phosphorylation and the development of tauopathies. *J Biol Chem*. 1999; 274:25490–25498. [PubMed: 10464280]
38. Adeghate E. Visfatin: Structure, function and relation to diabetes mellitus and other dysfunctions. *Curr Med Chem*. 2008; 15:1851–1862. [PubMed: 18691043]
39. Leger J, Kempf M, Lee G, Brandt R. Conversion of serine to aspartate imitates phosphorylation-induced changes in the structure and function of microtubule-associated protein tau. *J Biol Chem*. 1997; 272:8441–8446. [PubMed: 9079670]
40. Mandelkow EM, Biernat J, Drewes G, Steiner B, Lichtenberg-Kraag B, Wille H, Gustke N, Mandelkow E. Microtubule-associated protein tau, paired helical filaments, and phosphorylation. *Ann N Y Acad Sci*. 1993; 695:209–216. [PubMed: 7694533]
41. Biernat J, Gustke N, Drewes G, Mandelkow EM, Mandelkow E. Phosphorylation of ser262 strongly reduces binding of tau to microtubules: Distinction between phf-like immunoreactivity and microtubule binding. *Neuron*. 1993; 11:153–163. [PubMed: 8393323]

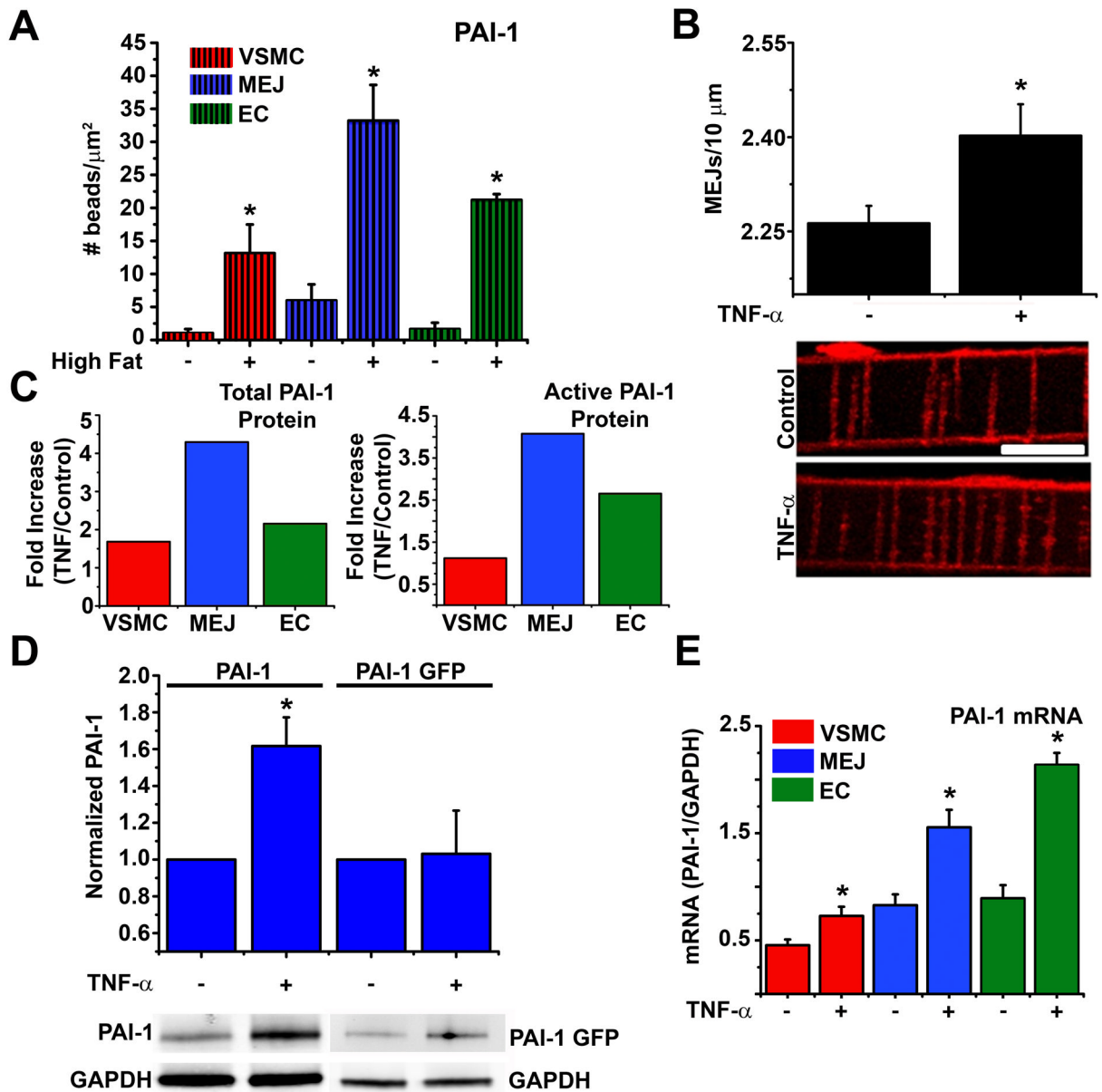


Figure 1. Characterization of PAI-1 and MEJ formation in response to a high fat diet or TNF- α
 The number of beads per micrometer squared for EC, VSMC and MEJs for normal (-) and high fat diet (+) is shown in A. Metamorph analysis of changes in the number of MEJs per 10 micrometers, following treatment with 10 ng/mL TNF- α to the EC monolayers is shown in (B, top). Representative images for confocal microscopy of transverse VCCC sections stained with phalloidin for control or TNF- α treated conditions are shown in (B, bottom). The fold increase for total PAI-1 (ng/mL) or active PAI-1 (units/mL) on isolated VCCC fractions, in response to TNF- α , was calculated using PAI-1 specific ELISAs (C). In D, increases in PAI-1 mRNA in response to TNF- α were quantified for isolated EC, VSMC, and MEJ fractions, using quantitative rt-PCR. Bar in B is 10 micrometers; statistical comparisons were made between each cellular compartment with $*=p<0.05$.

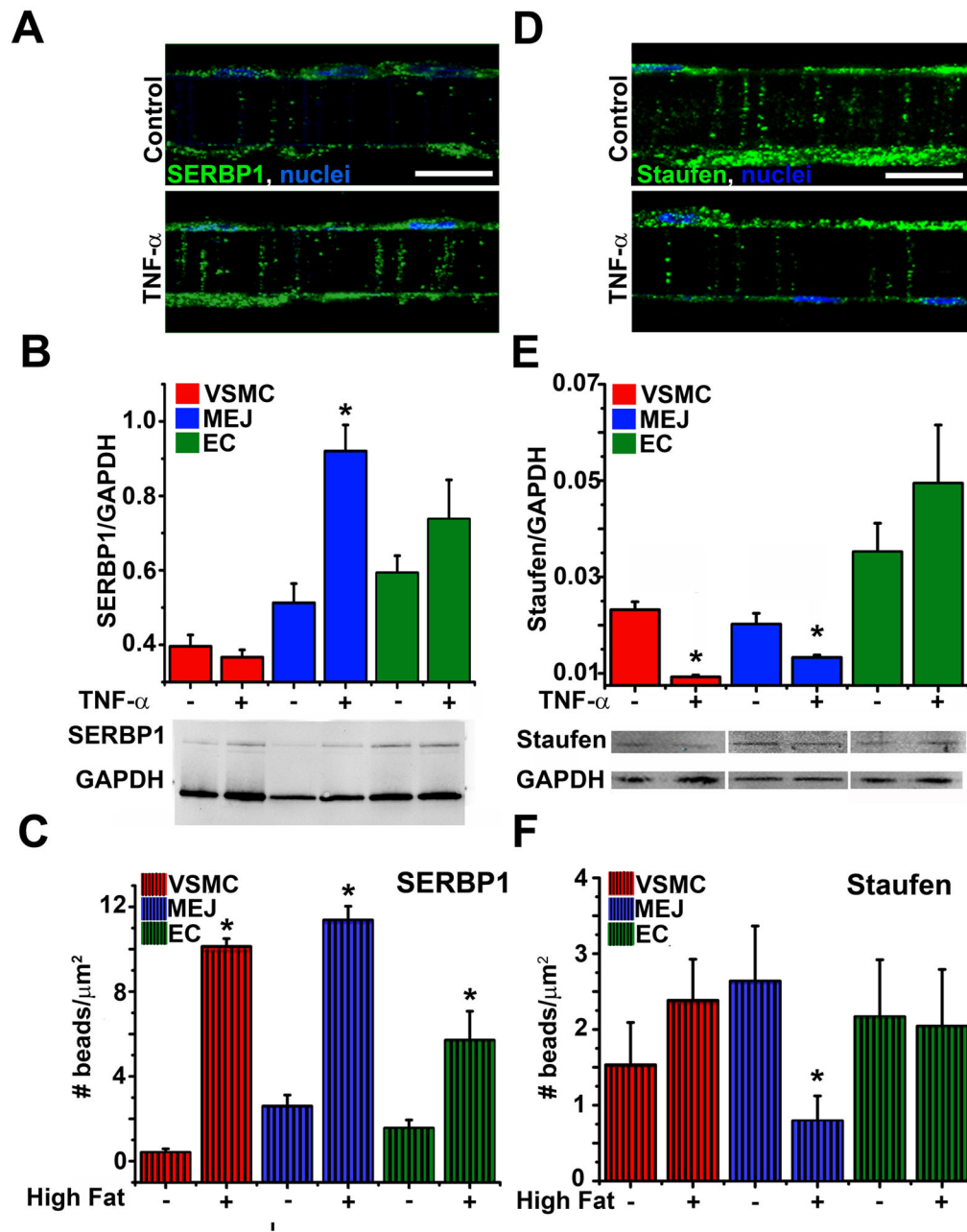


Figure 2. Effects of TNF- α or a high fat diet on SERBP1 and Staufen localization at the MEJ
 Transverse sections of VCCC sections stained for SERBP1 (green) and nuclei (blue), for control (A, top) or TNF- α (A, bottom) treated conditions demonstrates SERBP1 expression at the MEJ in response to TNF- α . In B, quantified immunoblots of VSMC, EC, and MEJ fractions isolated from the VCCC treated with (+) or without (-) TNF- α were blotted for SERBP1 and GAPDH as a loading control. In C, the expression of SERBP1 was quantified as the number of beads per micrometer squared for EC, VSMC, or MEJs. In D, transverse sections of VCCCs were stained for Staufen (green) and nuclei (blue), in control (D, top) or TNF- α (D, bottom) treated conditions demonstrates a lack of Staufen expression at the MEJ in response to TNF- α . In E, quantified immunoblots of VSMC, EC, and MEJ fractions isolated from the VCCC treated with (+) or without (-) TNF- α were blotted for Staufen and

GAPDH as a loading control. The expression of Staufen was quantified as the number of beads per micrometer squared for VSMC, EC or MEJs (F). Bars in A and D are 10 micrometers and for all graphs, statistical comparisons were made between each cellular compartment with $*=p<0.05$.

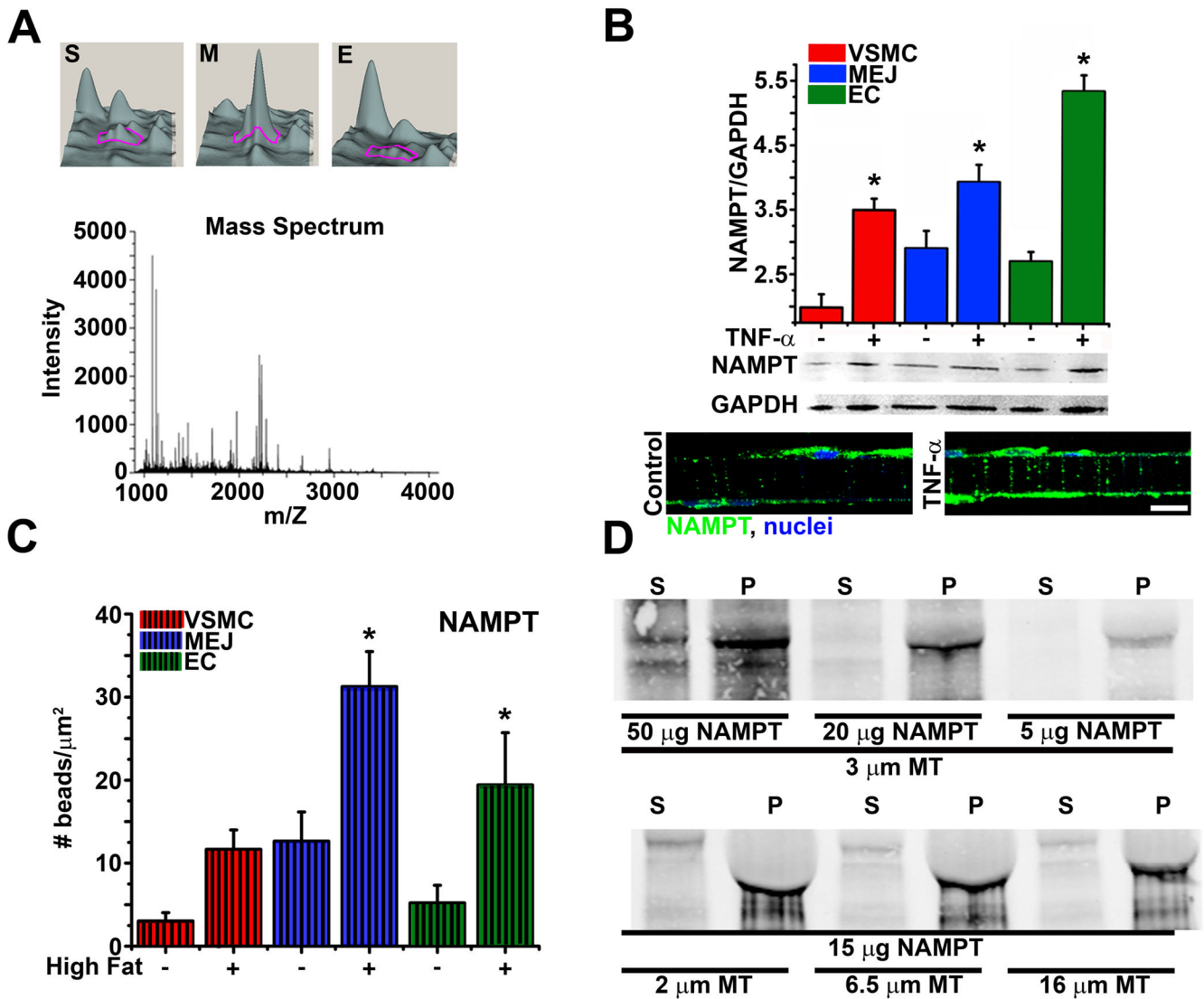


Figure 3. Characterization of NAMPT as a microtubule binding protein

In A, using Quantitative DeCyder analysis, a 3D visualization from a 2D-DIGE analysis compares a single protein expression, identified by a magenta tracer, between isolated VSMC (S), MEJ (M), or EC (E) VCCC fractions, with a minimum 2.5 fold increase in protein expression in the MEJ fractions compared to EC or VSMC. All three spots were identified as NAMPT using mass spectroscopy (A, bottom). Quantified immunoblots of VSMC, EC, and MEJ fractions isolated from VCCCs treated with (+) or without (-) TNF- α , probed for NAMPT are shown in B (top). Transverse sections of VCCCs stained for NAMPT (green) and nuclei (blue) for control (B, bottom left) and TNF- α (B, bottom right) treated conditions demonstrates changes in NAMPT expression in response to TNF- α . In C, the number of gold beads corresponding to NAMPT was quantified against each cellular part of the coronary vessel wall. Immunoblots probed for NAMPT on supernatant (S) and pellet (P) fractions from a co-sedimentation microtubule binding assay microtubules are shown in D. For D, experimental paradigms include maintaining the microtubule (MT) length at 3 micrometers with increasing amounts of purified rNAMPT at 5, 20 and 50 micrograms (top) and maintaining the amount of purified rNAMPT at 15 micrograms and increasing the length of microtubules at 2, 6.5 and 16 micrometers. The bar in B is 10

micrometers and in all graphs, statistical comparisons were made between each cellular compartment with $*=p<0.05$.

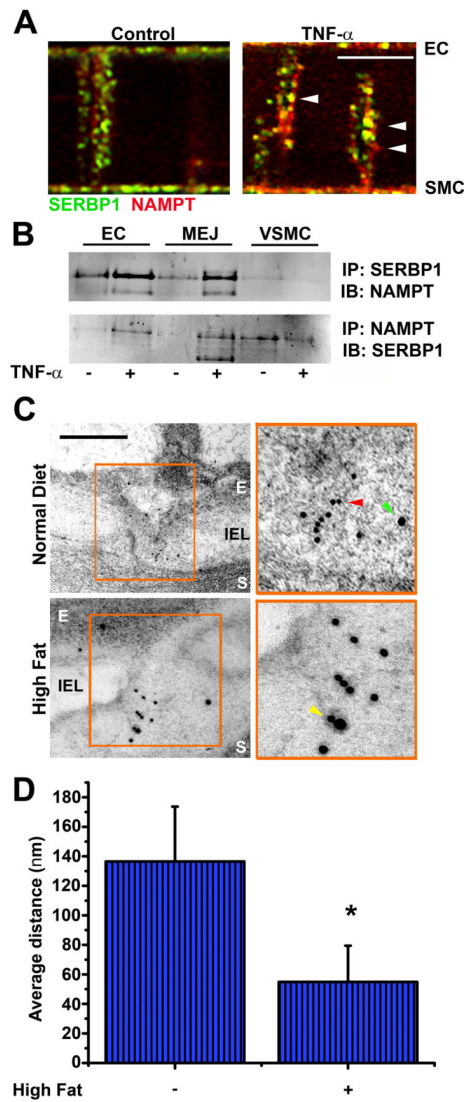


Figure 4. NAMPT and SERBP1 interact at the MEJ in vitro and colocalize at the MEJ, in vivo
 In A, co-immunostainings for SERBP1 (green) and NAMPT (red) on transverse sections of the VCCC are shown for control and TNF- α treated conditions. Interactions between SERBP1 and NAMPT were shown for isolated VCCC fractions by immunoprecipitating (IP) with SERBP1 (B, top) or NAMPT (B, bottom) and probing (WB) for NAMPT or SERBP1 respectively, with (+) or without (-) TNF- α . In C, representative TEM images of mouse coronaries from mice fed a normal (top) or high fat diet (bottom) are co-labeled for NAMPT using 10 nm gold beads (top enlargement, green arrowhead) and SERBP1 using 15 nm gold beads (top enlargement, red arrowhead). Colocalization of SERBP1 and NAMPT is shown in C (bottom enlargement, yellow arrowhead). In D, the distance between the 10 nm and 15 nm gold beads at the MEJ is averaged and compared between control and high fat conditions. In A, large arrows indicate single protein staining for SERBP1 (top arrow) or NAMPT (bottom arrow), white arrow heads indicate colocalization of SERBP1 and NAMPT. In C, “E” indicates endothelial cells, “S” indicates vascular smooth muscle cells. Bar in A is 5 micrometers, bars in C are 0.5 micrometers. In graph, statistical comparisons were made between each cellular compartment with $*=p<0.05$.

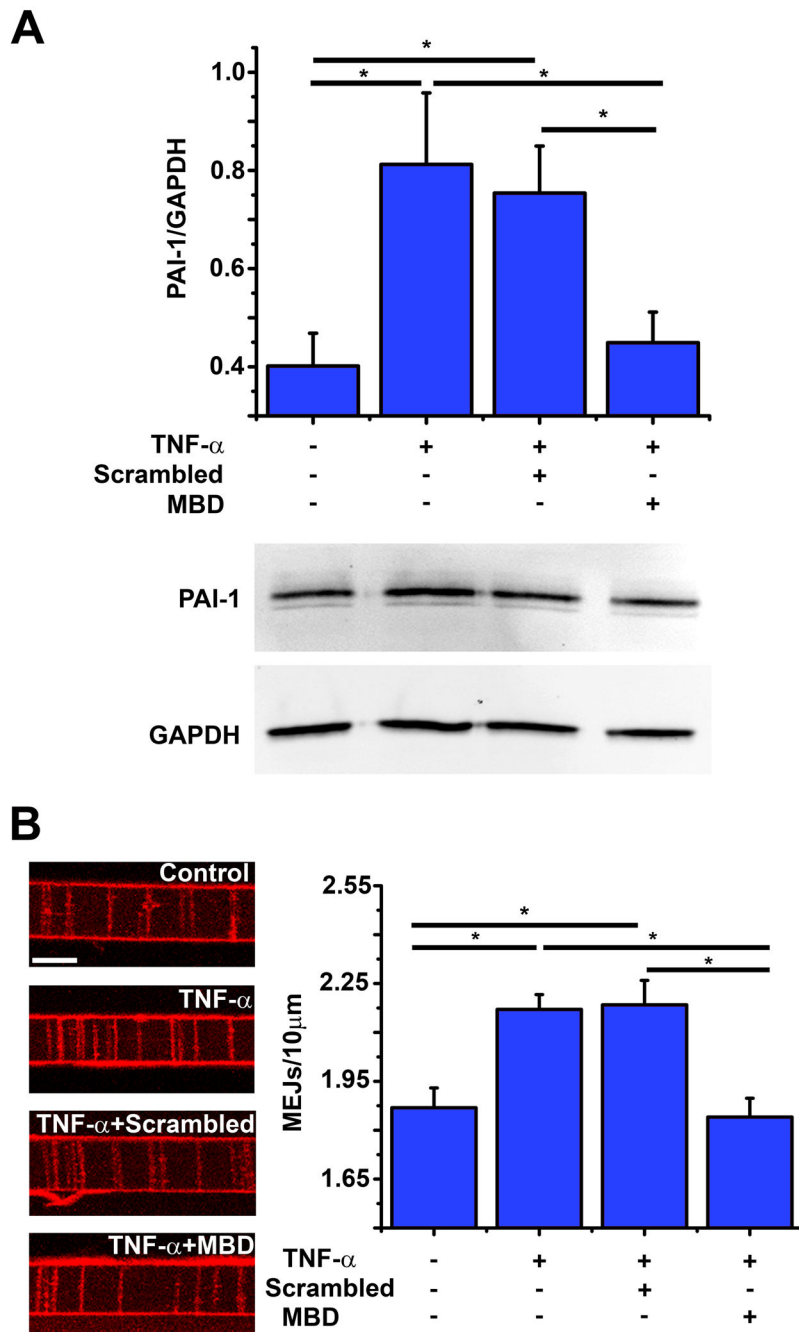


Figure 5. NAMPT anchoring is crucial for TNF- α induced increase in PAI-1 and MEJ formation, in vitro

A demonstrates quantitative immunoblot analysis of PAI-1 protein expression on isolated MEJ fractions for the following experimental paradigms, control (untreated), TNF- α (10 ng/mL), TNF- α + Scrambled peptide or TNF- α + MBD peptide. In B (left), the same experimental condition is shown for transverse sections of VCCCs stained with phalloidin. The number of MEJs for each paradigm was quantified and shown on right. Bar in B is 10 micrometers, * p <0.05.

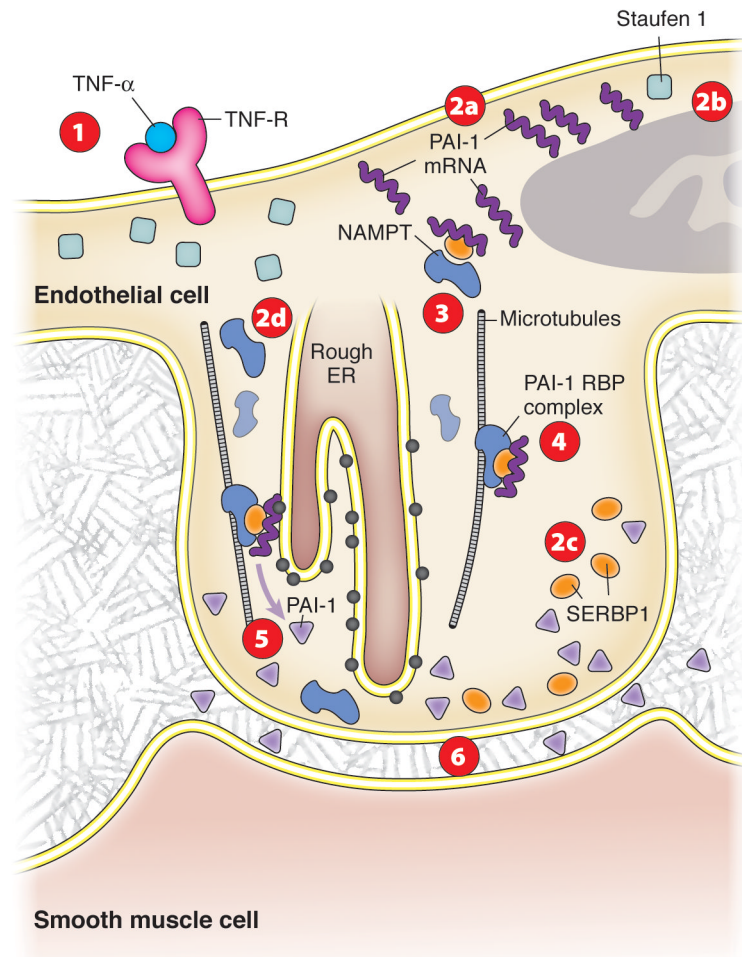


Figure 6. Localization of PAI-1 mRNA by NAMPT anchoring is crucial for PAI-1 expression at the MEJ and MEJ formation

Summary of PAI-1 mRNA localization. Application of inflammatory stimulation (TNF- α or high fat diet, 1) induces a global increase in PAI-1 mRNA (2a), decreases Staufen expression at the MEJ (2b) and increases NAMPT and SERBP1 expression at the MEJ (2c). This subcellular organization promotes the formation of a PAI-1 RBP-complex, comprised of PAI-1 mRNA, SERBP1 and NAMPT (3). The PAI-1 RBP complex is stabilized at the MEJ, via microtubule binding by NAMPT (4), which allows for the localized translation of PAI-1 protein at the MEJ (5) and subsequent increase in MEJ formation (6).